Available online at www.sciencedirect.com
SCIENCE DIRECT
Journal of Power Sources 155 (2006) 291–296
JOURNAL OF POWER SOURCES
www.elsevier.com/locate/jpowsour

Short communication

Experimental investigations of the anode flow field of a micro direct methanol fuel cell

C.W. Wong, T.S. Zhao *, Q. Ye, J.G. Liu

Department of Mechanical Engineering, The Hong Kong University of Science & Technology, Clear Water Bay, Kowloon, Hong Kong SAR, China

Received 4 March 2005; accepted 2 April 2005
Available online 27 June 2005

Abstract

The effect of the anode flow field design on the performance of an in-house fabricated micro direct methanol fuel cell (μDMFC) with an active area 1.0 cm × 1.0 cm was investigated experimentally. Single serpentine and parallel flow fields consisting of micro channels were tested. The experimental results indicated that the serpentine flow field exhibited significantly higher cell voltages than did the parallel flow field, particularly at high current densities. The study of the effect of channel depth of the serpentine flow field suggested that there exists an optimal channel depth for the same channel width and the same open ratio when the same methanol flow rate is supplied; either shallower or deeper channels will lead to a reduction in the cell performance. Finally, it was demonstrated that performance of the μDMFC with the reactants fed by an active means was insensitive to the cell orientations, which is different from conventional DMFCs with larger flow channels reported in the literature.

Keywords: Polymer electrolyte fuel cell; DMFC; Micro channel; Micro fuel cell

1. Introduction

The worldwide proliferation of portable electronic devices, including notebook and tablet computers, PDAs, camcorders, mobile phones and other power-hungry products, has created a large and growing demand for energy sources that are compact, lightweight and powerful. Existing rechargeable battery technology, which has greatly matured, simply does not meet the needs of users. This gap is expected to widen in the future, as devices become more powerful and full featured. Many industry observers have identified direct methanol fuel cells (DMFCs) as one of the most promising technologies that can bridge the power gap for portable electronics, primarily because DMFCs offer several unique features, such as their compact and lightweight systems, high power density and energy capacity, easy storage of liquid fuel, ambient temperature operation and without charging [1,2]. Although progress has been made over the last few years, significant technical challenges, including slow electrochemical kinetics of methanol oxidation, methanol cross-over through polymer membranes, cathode flooding, as well as CO_2 gas management, still remain barriers to commercialization of DMFCs. In order to circumvent these problems, efforts have been made to develop more active electrocatalysts [3–6], to modify and fabricate alternative membranes [7–15], to investigate water management on the cathode [16–19], as well as to study gas management on the anode of a DMFC [20–25].

In a DMFC, the anode flow field functions for supplying and distributing methanol solution on the anode electrode. The distribution of the fuel on the electrode surface should ideally be as uniform as possible to ensure a uniform performance across the electrode surface. The flow field allows methanol solution flow along the length of the electrode whilst permitting mass transport to the reaction layer (the catalyst layer) normal to its surface. In the catalyst layer, the electrochemical reaction of methanol oxidation produces CO_2, which is transferred backward, through the diffusion

* Corresponding author. Tel.: +852 2358 8647; fax: +852 2358 1543.
E-mail address: metzhao@ust.hk (T.S. Zhao).

0378-7753/$ – see front matter © 2005 Elsevier B.V. All rights reserved.
doi:10.1016/j.jpowsour.2005.04.028

layer, to the flow field. Therefore, another function of the anode flow field of a DMFC is to transport CO_2 out of the cell. In addition to the mass transfer resistance through the electrode itself, hydrodynamic mass transfer from the feed bulk flow to the surface of the electrode also affects the limiting current behavior of a DMFC. Therefore, a higher mass transfer rate at the interface between the flow field and the electrode is essential for improving the performance of DMFCs, which is generally affected by gas CO_2 evolution behavior in the flow field.

The anode flow field of conventional DMFCs with a relatively larger MEA has been studied extensively [20–25]. Aricò et al. [20] investigated both serpentine (SFF) and interdigital (IFF) flow fields with regard to their use in a DMFC. They found that SFFs showed lower methanol cross-over, higher fuel utilization and slightly larger voltage efficiency at low current densities, while IFFs enhanced mass transport and membrane humidification allowing to achieve high power densities of 450 and 290 mW cm^{-2} in the presence of oxygen and air feed, respectively, at 130 °C. Scott et al. [21] investigated visually the CO_2 bubble removal characteristics related to the cell performance under a number of the flow field designs based on stainless steel mesh. Amphlett et al. [22] investigated the performance of a DMFC equipped with parallel rectangular single-pass anode channels. Their experimental results indicated that the flow channel with a medium depth performed better than with either shallower or deeper channels. Bewer et al. [23] investigated the influence of the flow field on the bubble formation and on the flow homogeneity, as well as the influence of the manifold on the flow homogeneity with the aid of a novel method of simulating two-phase flow in a DMFC using an aqueous H_2O_2 solution. More recently, Yang and Zhao [24] studied the effect of the anode flow field design with single serpentine (SSFFs) and parallel (PFFs) flow fields on the performance of a DMFC. Their experimental results showed that the DMFCs equipped with the SSFFs yielded better performance than those with the PFFs. They observed that gas bubbles blocked the flow channels in the PFFs at low methanol solution flow rates and high current densities, but this channel-blocking phenomenon never happened in the SSFFs. They also found that both open ratio and flow channel length had significant influences on the cell performance and pressure drop in the SSFFs. Most recently, Wong et al. [25] investigated the CO_2 bubble evolution effect on the performance of an in-house fabricated μDMFC. They found that the anode flow channel was blocked by elongated gas slugs periodically when channel size was sufficiently small. And this transient channel blocking phenomenon has significant impact on the cell performance.

The objective of this work was to study the effect of the anode flow field design on the performance of a μDMFC with a rather small active area (1.0 cm × 1.0 cm). Both single serpentine and parallel flow fields were investigated and compared under the condition of the same channel width (500 μm), the same channel depth (500 μm) and the same open ratio (43%). The emphasis was then placed on the study of the effect of serpentine flow channel depth, being shrunk from 1.0 mm to 100 μm, on the performance of the μDMFC. Finally, the influences of aqueous methanol solution flow rates and cell orientation were also examined in this work.

2. Experimental

2.1. The micro cell

The μDMFC designed and fabricated for this study is shown in Fig. 1. It consisted of a membrane electrode assembly (MEA) sandwiched between two stainless steel plates with a machined flow field, which were clamped by two aluminum fixtures through four M5 screw joints with torque of 1 N m. Teflon tapes were used as the sealing material for the MEA. The operating temperature was controlled by two heating rods installed in the aluminum fixtures and connected to a temperature controller (Digi-Sense®).

The MEA (1.0 cm × 1.0 cm active area) consisted of two single-side ELAT electrodes purchased from E-TEK and a Nafion® 115 membrane with pretreatment. The carbon cloth (E-TEK, Type A) with 30% PTFE wet-proofing treatment was used as the backing support layer in the anode and cathode electrodes. 4.0 mg cm^{-2} with unsupported [Pt:Ru] Ox (1:1 a/o) and 2.0 mg cm^{-2} using 40% Pt on Vulcan XC-72 were used as the catalyst loading on the anode and cathode side. Furthermore, 0.8 mg cm^{-2} Nafion® was applied onto the catalyst layer surface of each electrode. The pretreatment of Nafion® 115 membrane was followed the standard procedure before being used: (a) boiling membrane in 5 wt.% H_2O_2 solution at 80 °C for 1 h; (b) rinsing with DI water at 80 °C for 1 h; (c) boiling membrane in 0.5 M H_2SO_4 solution at 80 °C for 1 h and (d) rinsing with DI water at 80 °C for 1 h. Finally, the MEA was formed by hot press process under the condition of 135 °C and 4 MPa for 2 min.

2.2. Flow field design

Both single serpentine and parallel flow fields were tested in this work. The geometry parameters of the flow fields are

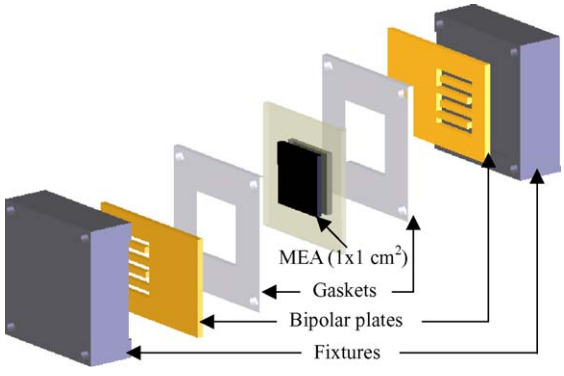

Fig. 1. Schematic of the in-house fabricated μDMFC.

Table 1
Geometric parameters of the anode flow fields

Flow fields	Parallel	Serpentine					
Channel width (μm)	500	500	580	580	580	580	580
Channel depth (μm)	500	500	1000	500	300	200	100
Rib width (μm)	500	500	470	470	470	470	470
Hydraulic diameter (μm)	500	500	734	537	395	297	171
Cross-section area (mm^2)	0.25×10	0.25	0.58	0.29	0.17	0.12	0.06
Open ratio (%)	43	43	49	49	49	49	49
Re (at 0.8 ml min^{-1} and 60 °C)	5.6	55.8	35.3	51.7	63.4	71.5	82.0
Internal resistance (Ω cm^2) at 30 °C	0.300	0.302	0.349	0.346	0.342	0.368	0.379
Internal resistance (Ω cm^2) at 60 °C	0.226	0.230	0.252	0.258	0.257	0.271	0.280

listed in Table 1. The comparison tests between the two flow fields were carried out under the condition of the same channel width (500 μm), the same channel depth (500 μm) and the same open ratio (43%). Experiments were then performed by investigating the channel depth effect under the condition of the same channel width (580 μm) and the same open ratio (49%), but varying channel depth from 1.0 mm to 500 μm, 300 μm, 200 μm and 100 μm. The flow of methanol solution in the anode flow channel can be characterized by the Reynolds number (*Re*) defined as:

$$Re = \frac{\rho Q_{in} D}{\mu A} \quad (1)$$

where ρ is the density of methanol solution, Q_{in} the methanol solution flow rate at the inlet of flow channel, D the hydraulic diameter of flow channel, μ the viscosity of methanol solution and A is the cross-section area of flow channel. The Reynolds numbers corresponding to each flow field design at $Q_{in} = 0.8$ ml min^{-1} are also listed in Table 1.

To avoid corrosion, the bipolar plates were made of 316L stainless steel. To reduce the electrical resistance, the bipolar plates were electroplated with a thin layer of gold (0.1 μm). All the flow fields were fabricated onto the bipolar plates by wire-cut technique. An interdigital flow field with 500 μm channel width and 500 μm channel depth was used on the cathode side in this work.

2.3. Test rig

The experiments were carried out in a test rig detailed elsewhere Yang and Zhao [24]. One molar aqueous methanol solution as the fuel was driven by a digital HPLC micro pump (Series III) with the range from 0.01 to 10.0 ml min^{-1} flow rate under an error of 2% of reading. At methanol solution flow rates (above 10 ml min^{-1}), a digital HPLC micro pump (Series II) with the range from 0.1 to 40.0 ml min^{-1} volume flow rate with the same error was used. Methanol solution was preheated by an in-house fabricated heater controlled by the temperature controller (Digi-Sense®) before enter the inlet of the cell. The mixture of CO_2 and unreacted methanol solution were drained from the outlet of the cell and collected into a liquid tank. On the cathode side, 99.999% high purity oxygen as the oxidant was supplied from the cylinder without humidification simultaneously. The mass flow meter (Omega FMA-7105E) combined with a multiple channel indicator (Omega FMA-5876A) were used to control and measure the flow rate of oxygen before it entered into the inlet of the cell, with flow rates ranging from 5 to 500 standard cubic centimeter per minute (SCCM) under an error of 1% of the full scale. The water and the excess oxygen gas were released from the outlet of cathode side and collected into a liquid tank.

2.4. Electrochemical instrumentation and test conditions

An Arbin BT2000 (Arbin Instrument) electro-load interfaced with a computer was employed to control the cell operation condition and to measure voltage–current (polarization) curves of the fuel cell. All the experiments were under controlled by the schedule program which testing from zero (open circuit status) to higher discharged current incrementally.

In this paper, all the experiments were performed under the same cathode operation condition with a constant oxygen gas flow rate of 10 SCCM at atmospheric pressure. One molar aqueous methanol solution was used in all the experiments.

3. Results and discussion

3.1. Comparison between the serpentine and parallel flow fields

Fig. 2 compares the performance of the cells with the serpentine and the parallel flow fields, which had the same channel width (500 μm), the same channel depth (500 μm) and 43% open ratio. The experiments were performed with 1 M methanol fed at 0.8 ml min^{-1} at 30 °C (Fig. 2a) and 60 °C (Fig. 2b). The corresponding Reynolds number is 5.6 for the parallel flow field and 55.8 for the serpentine flow field. It is clear from Fig. 2a and b that for the same methanol solution flow rate, the serpentine flow field exhibited much higher performance than the parallel flow field, particularly at high current densities. The improved performance with the serpentine flow field is primarily attributed to the fact that at the same methanol solution flow rate the liquid velocity (or the Reynolds number) in the serpentine flow field was much

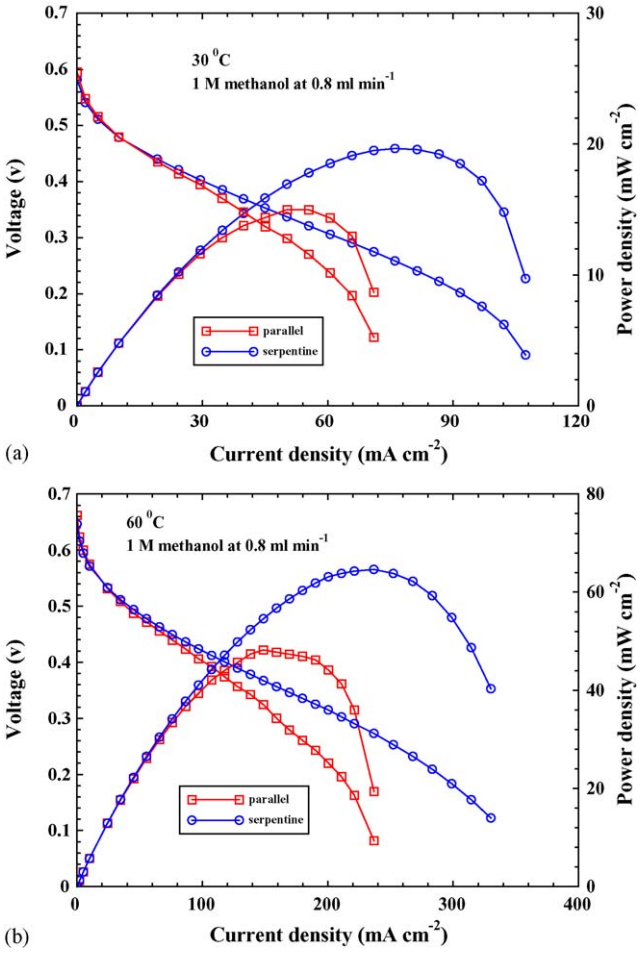

Fig. 2. Polarization and power density curves of the cell with either the serpentine or the parallel flow field with 1 M methanol fed at 0.8 ml min^{-1} at: (a) 30 °C and (b) 60 °C.

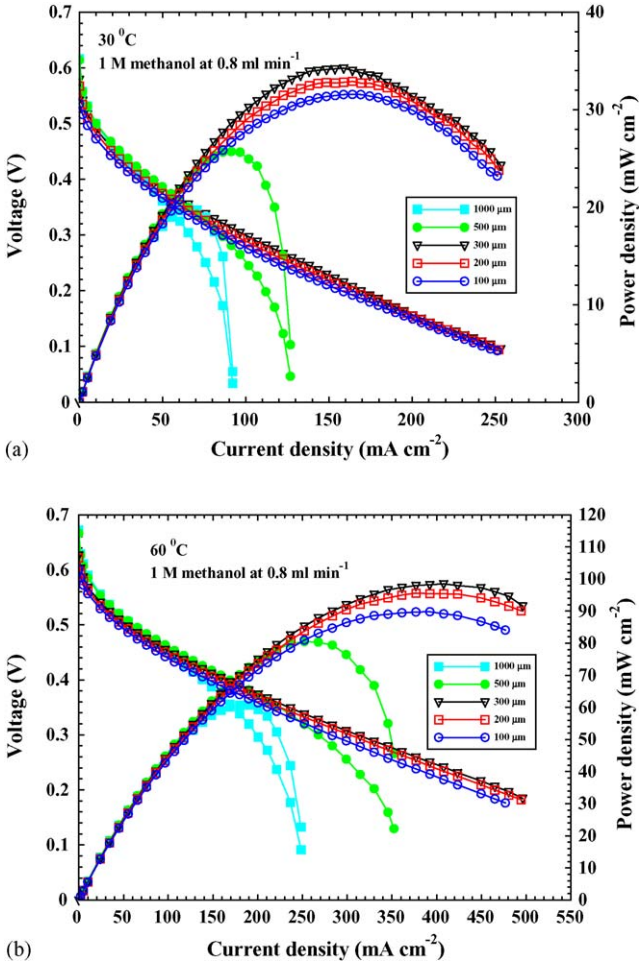

Fig. 3. Effect of serpentine flow channel depth on the performance with 1 M methanol fed at 0.8 ml min^{-1} at: (a) 30 °C and (b) 60 °C.

higher than in the parallel flow field, as the channel cross-sectional area in the serpentine flow channel was 10 times smaller than in the parallel flow channels (see Table 1). The higher liquid velocity (or larger Reynolds number) enhances the mass transfer of methanol from the flow channel to the gas diffusion layer, thereby improving the cell performance [26]. It is observed that the peak power density with the serpentine flow field was increased by about 31.3% at 30 °C and 34.0% at 60 °C compared to the parallel flow field.

3.2. The influence of serpentine flow channel depth

Fig. 3 presents the channel depth effect of the serpentine flow field with the same channel width (580 μm) and the same open ratio (49%) on the cell performance. The experiments were conducted with 1 M methanol solution fed at a flow rate of 0.8 ml min^{-1} and at 30 °C (Fig. 3a) and at 60 °C (Fig. 3b). The Reynolds numbers corresponding to the channel depths of 1.0 mm, 500 μm, 300 μm, 200 μm and 100 μm are 35.3, 51.7, 63.4, 71.5 and 82.0, respectively. It is seen from Fig. 3b that the performance was upgraded drastically as channel depth was reduced from 1.0 mm to 500 μm and 300 μm. A further reduction in channel depth from 300 to 200 μm and 100 μm, however, caused the performance to degrade. The 300 μm channel depth exhibited the best performance among all the channels tested, achieving a peak power density of around 100 mW cm^{-2}. The channel depth effect at a lower operating temperature (30 °C), presented in Fig. 3a, shows that the performance varied in a similar fashion to that presented Fig. 3b at a higher operating temperature; again, the 300 μm channel depth yielded the best performance. Fig. 4 presents the variation in the peak power density with channel depth. It is observed that at 30 °C, the peak power density was increased by about 71.9% when channel depth was reduced from 1.0 mm to 300 μm; it was, however, decreased by 8.6% when channel depth was further reduced to 100 μm. Similarly, at 60 °C, the peak power density was found to increase by 62.1% when channel depth was reduced from 1.0 mm to 300 μm; it was decreased by about 9.7% when channel depth was further reduced to 100 μm. It is worth mentioning that the change in the cell internal resistance with channel depth was rather small, as can be seen from Table 1.

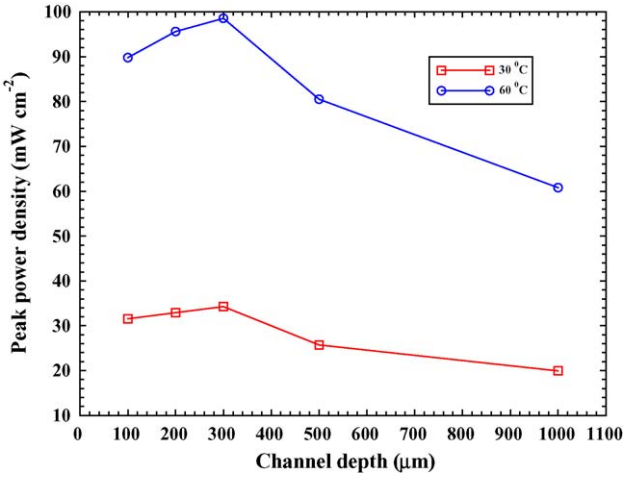

Fig. 4. Effect of serpentine flow channel depth on the peak power density with 1 M methanol fed at 0.8 ml min^{-1} and at 30 °C and 60 °C.

The above results on the channel depth effect indicate that there exists an optimal channel depth for the same channel width and the same open ratio when the same methanol flow rate is supplied; either shallower or deeper channels will lead to a reduction in the cell performance. This performance variation behavior with channel depth can be explained as follows. Our previous studies [25] have shown that in the serpentine flow channel the gas void fraction increases along channel length, the liquid flow can never be fully developed. Under such a circumstance, the mass transfer coefficient is the function of the liquid flow velocity (or Reynolds number); a higher flow velocity will lead to a higher mass transfer coefficient. Since for the same flow rate the liquid velocity increases with decreasing channel depth, a smaller channel depth will yield a higher mass transfer rate. This explains why the 300 μm channel depth led to a better performance than did the 1.0 mm and 500 μm channel depths.

On the other hand, the mass transfer rate also depends on the effective mass transfer area between the bulk methanol solution and the surface of the diffusion layer. The effective mass transfer area is strongly affected by the CO_2 bubble evolution behavior in flow channels. Our previous visual study [25] of CO_2 bubble behavior revealed that in a sufficiently small flow channel, the bubble evolution and removal from the flow field were undergoing in a cyclic manner caused by the so-called transient capillary blocking. It has been shown that the residence time of elongated gas slugs in the channel became longer as the channel size was reduced. As such, the effective mass transfer area at the surface of the diffusion layer becomes smaller with a reduction in channel depth. Therefore, a too shallow flow channel will lead to a too small effective mass transfer area, hence a lower mass transfer rate, which in turn causes the cell performance to decline. This explains why the serpentine flow channels with 100 and 200 μm depth exhibited lower performance than did the flow channel with 300 μm depth, as shown in Fig. 3.

In summary, for the same methanol solution flow rate, flow channels with smaller depth will lead to higher mass transfer coefficient, which is a favorable effect on the cell performance. On the other hand, the longer gas slugs in flow channels with smaller depth yield a smaller effective mass transfer area between the methanol solution and the diffusion layer. In this context, smaller channel depths will affect the cell performance adversely. The competition between the higher mass transfer coefficient and the smaller effective mass transfer area results in an optimal channel size that gives the best cell performance. For the presently-configured MEA operated with 1 M methanol at 0.8 ml min^{-1}, this optimal channel depth was 300 μm for the channel width of 580 μm.

3.3. The influence of cell orientation

Fig. 5 shows the orientation effect on the performance of the cell with the serpentine flow channel having a depth of 500 μm and a width of 580 μm. The experiments were performed at 60 °C with 1 M methanol solution fed at flow rates of 0.1 ml min^{-1} (Fig. 5a) and 0.8 ml min^{-1} (Fig. 5b). The cell

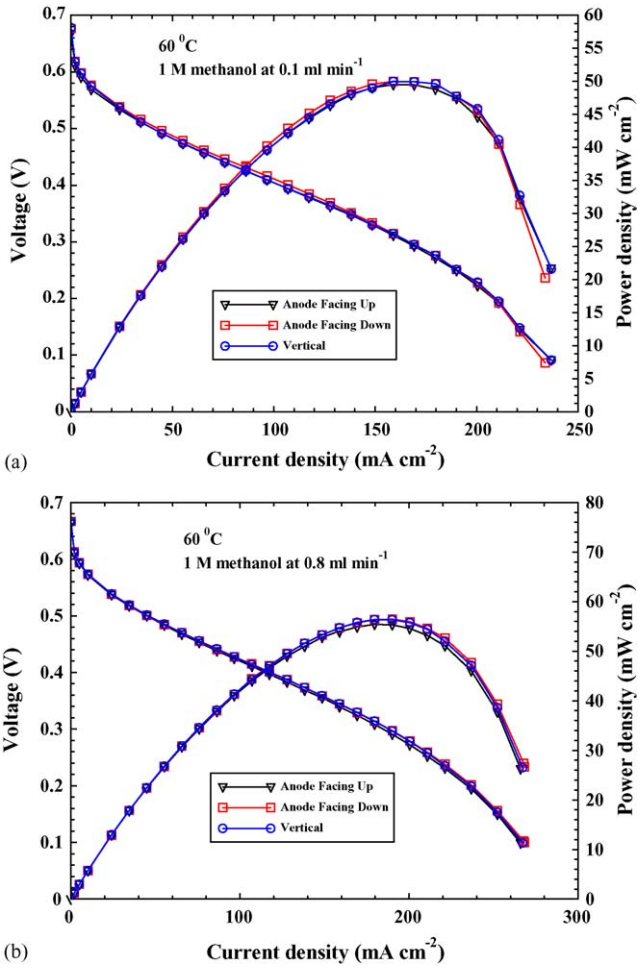

Fig. 5. Effect of the cell orientation on the performance for the serpentine flow channel (500 μm in depth and 580 μm in width) at 60 °C and with 1 M methanol fed at: (a) 0.1 ml min^{-1} and (b) 0.8 ml min^{-1}.

orientation changed from vertical to horizontal with either the anode facing up or facing down. It is interesting to notice that the performance remained almost unchanged when the cell orientation was changed, although the flow rate was as low as 0.1 ml min^{-1}, suggesting that the present μDMFC is insensitive to the cell orientations. This behavior is different from that for the DMFC with a larger active area (4 cm × 4 cm) and flow channel (2 mm × 2 mm) reported elsewhere [27], which showed that the orientation had a significant effect on the cell performance and the best performance was achieved for the vertical orientation. The reason why the performance of the μDMFC is insensitive to the cell orientations might be attributed to the fact that the capillary force becomes more important than buoyancy when the flow channel is sufficiently small.

4. Conclusions

The effect of the anode flow field design on the performance of an in-house fabricated μDMFC with an active area 1.0 cm × 1.0 cm has been investigated experimentally. Salient finds of this work can be summarized as follows:

(1) The comparison in performance between the serpentine and parallel flow fields indicates that the former yielded much higher performance than did the latter, particularly at high current densities.
(2) The study of the effect of channel depth of the serpentine flow field suggests that there exists an optimal channel depth for the same channel width and the same open ratio when the same methanol flow rate is supplied; either shallower or deeper channels will lead to a reduction in the cell performance. For the presently configured MEA operated with 1 M methanol at 0.8 ml min^{-1}, this optimal channel depth was 300 μm for the channel width of 580 μm.
(3) It was found that performance of the μDMFC with the fuel and oxygen fed by an active means was insensitive to the cell orientations, which is different from conventional DMFCs with larger flow channels reported in the literature.

Acknowledgement

The work described in this paper was fully supported by a grant from the Research Grants Council of the Hong Kong Special Administrative Region, China (Project No. HKUST6101/04E).

References

[1] C.K. Dyer, J. Power Sources 106 (2002) 31.
[2] J. Larminie, A. Dicks, Fuel Cell Systems Explained, second ed., Wiley, Chichester, West Sussex, 2003.
[3] B. Gurau, R. Viswanathan, R. Liu, T.J. Lafrenz, K.L. Ley, E.S. Smotkin, E. Reddington, A. Sapienza, B.C. Chan, T.E. Mallouk, S. Sarangapani, J. Phys. Chem. B 102 (1998) 9997.
[4] L. Liu, C.P. Cong, R. Viswanathan, Q. Fan, R. Liu, E.S. Smotkin, Electrochim. Acta 43 (1998) 3657.
[5] J.H. Choi, K.W. Park, I.S. Park, W.H. Nam, Y.E. Sung, Electrochim. Acta 50 (2004) 787.
[6] M. Carmo, V.A. Paganin, J.M. Rosolen, E.R. Gonzalez, Alternative supports for the preparation of catalysts for low-temperature fuel cells: the use of carbon nanotubes, J. Power Sources 142 (2005) 169.
[7] N. Yoshida, T. Ishisaki, A. Watakabe, M. Yoshitake, Electrochim. Acta 43 (1998) 3749.
[8] E. Peled, T. Duvdevani, A. Melman, Electrochem. Solid-State Lett. 1 (1998) 210.
[9] B.S. Pivovar, Y. Wang, E.L. Cussler, J. Membr. Sci. 154 (1999) 155.
[10] P. Staiti, M. Minutoli, S. Hocevar, J. Power Sources 90 (2000) 231.
[11] N. Jia, M.C. Lefebvre, J. Halfyard, Z. Qi, P.G. Pickup, Electrochem. Solid-State Lett. 3 (2000) 529.
[12] B. Libby, W.H. Smyrl, E.L. Cussler, Electrochem. Solid-State Lett. 4 (2001) A197.
[13] F. Finsterwalder, G. Hambitzer, J. Membr. Sci. 185 (2001) 105.
[14] Z.Q. Ma, P. Cheng, T.S. Zhao, J. Membr. Sci. 215 (2003) 327.
[15] Y.S. Kima, M.A. Hicknerc, L. Dongd, B.S. Pivovara, J.E. McGrathb, J. Membr. Sci. 243 (2004) 317.
[16] X. Ren, T.E. Springer, S. Gottesfeld, J. Electrochem. Soc. 147 (2000) 92.
[17] M.M. Mench, C.Y. Wang, J. Electrochem. Soc. 150 (2003) A79.
[18] A. Blum, T. Duvdevani, M. Philosoph, N. Rudoy, E. Peled, J. Power Sources 117 (2003) 22.
[19] G.Q. Lu, C.Y. Wang, J. Power Sources 134 (2004) 33.
[20] A.S. Aricò, P. Creti, V. Baglio, E. Modica, V. Antonucci, J. Power Sources 91 (2000) 202.
[21] K. Scott, P. Argyropoulos, P. Yiannopoulos, W.M. Taama, J. Appl. Electrochem. 31 (2001) 823.
[22] J.C. Amphlett, B.A. Peppley, E. Halliop, A. Sadiq, J. Power Sources 96 (2001) 204.
[23] T. Bewer, T. Beckmann, H. Dohle, J. Mergel, D. Stolten, J. Power Sources 125 (2004) 1.
[24] H. Yang, T.S. Zhao, Effect of anode flow field design on the performance of liquid feed direct methanol fuel cells, Electrochim. Acta 50 (2005) 3243.
[25] C.W. Wong, T.S. Zhao, Q. Ye, J.G. Liu, Transient capillary blocking in the flow field of a micro DMFC and its effect on cell performance, J. Electrochem. Soc., in press.
[26] H. Yang, T.S. Zhao, Q. Ye, Electrochem. Commun. 6 (2004) 1098.
[27] H. Yang, T.S. Zhao, Q. Ye, J. Power Sources 139 (2005) 79.